Protection of Gypenoside XVII against cerebral ischemia/reperfusion injury across the SIRT1-FOXO3A and Hif1a-BNIP3-mediated mitochondrial autophagy

jie Wei Xie
Chinese Academy of Medical Sciences & Peking Union Medical College Institute of Medicinal Plant Development
Ting Zhu
Qingdao University
xia Shu Zhang
Chinese Academy of Medical Sciences & Peking Union Medical College Institute of Medicinal Plant Development
bo Xiao Sun (sun-xiaobo@163.com)
Chinese Academy of Medical Sciences & Peking Union Medical College Institute of Medicinal Plant Development

Research Article

Keywords: Gypenoside XVII, cerebral ischemia/reperfusion injury, FOXO3A, BNIP3, mitochondria autophagy

Posted Date: August 1st, 2022

DOI: https://doi.org/10.21203/rs.3.rs-1880338/v1

Protection of Gypenoside XVII against cerebral ischemia/reperfusion injury across the SIRT1-FOXO3A and Hif1a-BNIP3-mediated mitochondrial autophagy

Weijie Xie[1,2,3,5*], Ting Zhu[1,2,3,4*], Shuxia Zhang[1,2,3], Xiaobo Sun[1,2,3]

[1] *Institute of Medicinal Plant Development, Peking Union Medical College and Chinese Academy of Medical Sciences, Beijing 100193, China;*

[2] *Key Laboratory of Material Basis and Resource Utilization of Chinese Herbal Medicine, Beijing 100193, China;*

[3] *State Administration of Traditional Chinese Medicine Key Laboratory of Efficacy evaluation of Traditional Chinese Medicine in intervention of disorders of glucose and Lipid Metabolism, Beijing 100193, China;*

[4] *Institute of Neuroregeneration & Neurorehabilitation, Department of Pathophysiology, School of Basic Medicine, Qingdao University, Qingdao 266071, China;*

[5] *Shanghai Mental Health Centre, School of Medicine, Shanghai Jiao Tong University, Shanghai 200011, China*

*These authors contributed equally to this work.

Corresponding author: Xiaobo Sun, Research Center for Pharmacology and Toxicology, Institute of Medicinal Plant Development, Chinese Academy of Medical Sciences and Peking Union Medical College, Malianwa North Road 151, Beijing, 100193, China. E-mail addresses: sun-xiaobo@163.com (XB Sun).

Abstract

Background: Mitochondrial autophagy maintains mitochondrial function and cellular homeostasis, and plays a critical role in the pathological process of cerebral ischemia/reperfusion injury (CIRI). Whether Gypenoside XVII (GP17) has regulatory effects on mitochondrial autophagy against CIRI remains unclear. The purpose of this study was to investigate the pharmacodynamic effect and mechanism of GP17 on mitochondrial autophagy after CIRI.

Methods: A rat model exposed to middle cerebral artery occlusion/reperfusion (MCAO/R) was used to assess the effects of GP17 against CIRI and to explore the underlying mechanisms. The oxygen-glucose deprivation/reoxygenation (OGD/R) cell model was used to verify the effects of ameliorating mitochondria damages and to probe the autophagy pathways of combating neural injuries.

Results: The in vivo results shows that GP17 significantly improves mitochondrial metabolic functions and suppresses cerebral ischemia injuries, which might be involved in the autophagy pathway. The further researches reveal that GP17 maintains the moderate activation of autophagy under the ischemia and OGD conditions, producing neuroprotective effects again CIRI, and the regulation of mitochondrial autophagy is associated with a crosstalk between SIRT1-FOXO3A and Hif1a-BNIP3

signaling pathways, which are partially eliminated by special inhibitors AGK-7 and 2-ME.

Conclusions: Overall, this work offers new insights for exploring mechanisms by which GP17 protects against CIRI, and highlights the potential that therapy with Notoginseng leaf triterpenes as a novel clinical drug in humans.

Keywords: Gypenoside XVII; cerebral ischemia/reperfusion injury; FOXO3A; BNIP3; mitochondria autophagy

Abbreviations: CIRI, cerebral ischemia/reperfusion injury; GP17, gypenoside XVII; MCAO/R, middle cerebral artery occlusion/reperfusion; OGD/R, oxygen-glucose deprivation/reoxygenation; NAMPT, nicotinamide phosphoribosyltransferase; NBP, dl-3-n-butylphthalide; TTC, triphenyltetrazolium chloride; MMP, mitochondrial membrane potential.

Introduction

Stroke, especially ischemic stroke, is one of the leading causes of death worldwide. It is mainly caused by cerebral ischemia/reperfusion injury (CIRI). In the early stage of ischemia, ischemia causes insufficient NAD^+ levels and a decrease in the ratio of NAD^+/NADH, which directly impairs H^+ transmission in the oxidative respiratory chain and results in insufficient intracellular ATP synthesis, thus leading to mitochondrial damage and energy metabolism disorders [1-3]. Nicotinamide phosphoribosyltransferase (NAMPT) is a rate-limiting enzyme in the NAD synthesis pathway in humans [4]. Currently, it is reported that NAMPT can increase ischemic tolerance and improve mitochondrial energy metabolism during ischemia, suggesting that NAMPT may be a key target for the prevention and treatment of ischemic stroke. Therefore, among the popular research topics is finding natural active substances and compounds that can effectively inhibit mitochondrial damage and alleviate neuronal apoptosis and necrosis, as well as exploring their mechanism with respect to NAMPT targets for the prevention and treatment of ischemic stroke.

Autophagy is a conservative process of cellular self-digestion and catabolism, through which lysosomes are responsible for degrading damaged proteins and organelles to maintain cellular homeostasis and normal function [5, 6]. As one of the

87 homeostasis regulation mechanisms in vivo, autophagy has been shown to participate
88 in the entire process of ischemic stroke through pathways such as PKC/JNK,
89 PI3K/AKT-mTOR, and AMPK/mTORC1 [6, 7]. Under ischemic and hypoxic
90 conditions, autophagy is important for maintaining intracellular environmental
91 stability and self-renewal ability, as it removes damaged organelles and abnormal
92 proteins in cells. Thus, the regulation of autophagy is regarded as one of the key
93 strategies against CIRI.

94 Due to the complexity of the pathogenesis of ischemic stroke, the limitations of
95 therapeutic drugs and the major international and domestic needs, an increasing
96 number of researchers have studied traditional Chinese medicine as an important way
97 to treat ischemic stroke [8, 9]. Notoginseng leaf triterpenes (PNGL), a total saponin of
98 Panax notoginseng stems and leaves, attenuates neuronal apoptosis [10] and
99 ameliorates mitochondrial oxidative injury caused by ischemia [11, 12]. Gypenoside
100 XVII (GP17, the chemical structure is shown in Figure 1A), a unique component of
101 PNGL, exhibits many pharmacological effects through the suppression of endothelial
102 apoptosis, oxidative stress [13] and endoplasmic reticulum stress-induced
103 mitochondrial injury [14]. Our previous studies mainly demonstrated that GP17
104 attenuates Aβ25–35-induced parallel autophagic and apoptotic cell death [15].

Moreover, GP17 can enhance lysosome biogenesis and accelerate autophagic clearance of amyloid-β through TFEB activation [16], but its neuroprotective role in regulating autophagy has not been investigated in ischemic stroke.

The mechanisms by which GP17 regulates mitochondrial protection in the NAMPT-mediated pathway were elucidated previously [11, 12]. The present study further focused the downstream of its mediated pathways. In this work, we evaluated the effects of GP17 on CIRI in middle cerebral artery occlusion/reperfusion (MCAO/R)-treated rats and oxygen-glucose deprivation/reoxygenation (OGD/R)-treated SH-SY5Y cells. The purpose of this study was to illuminate the regulatory effects of GP17 on mitochondrial damages and autophagy after ischemic stroke.

Results

GP17 reduces cerebral infarction, neurological deficit scores and neuronal pathological damage in rats after ischemia

In the therapeutic efficacy study on MCAO/R rats, GP17 pretreatment at 10 and 20 mg/kg notably decreased the Longa scores and Bederson scores 24 h after ischemia (Figure 1B, C). In agreement, GP17 at 10 and 20 mg/kg given i.p. 7 days before ischemia significantly reduced the infarct volume (Figure 1D, E). GP17 (20

mg/kg)-treated rats exhibited neurological deficit scores similar to those of NBP-treated rats. Accordingly, GP17-treated rats displayed a better recovery of body weight than that of MCAO/R rats (Figure 1F). At a dose of 20 mg/kg, GP17 also reduced the pyknotic nuclei in the cortex (Figure 1G, H) and hippocampal (Figure 1G, I) regions.

In addition, GP17 (20 mg/kg) pretreatment significantly reduced the expression levels of the inflammatory cytokines IL-6, TNF-α, and MCP-1 and the oxidative cytokines T-AOC and 4-HNE (Figure S1A-E).

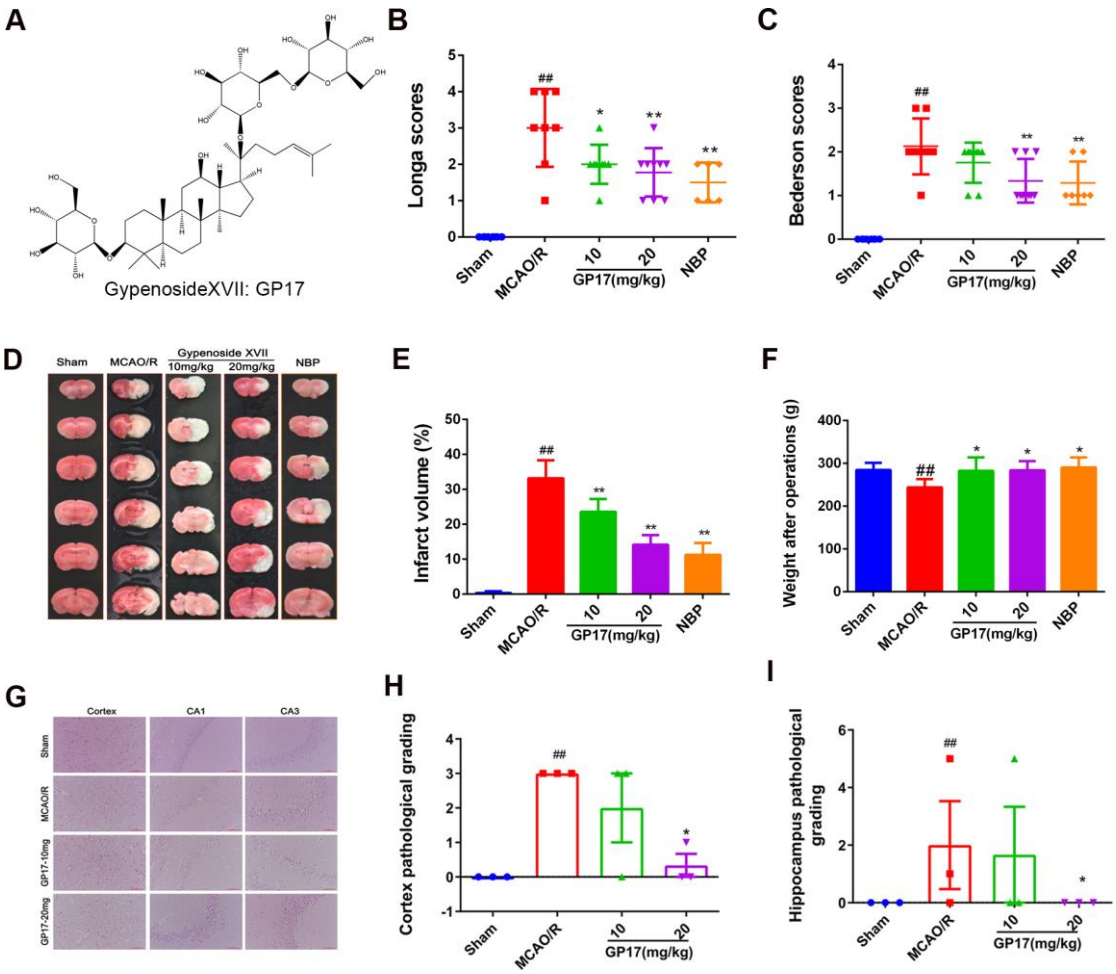

Fig. 1. Effects of GP17 on infarct volume, neurological deficit scores and neuronal

pathological changes in MCAO/R injury rats. A. Chemical structure of GP-17. B and C. Neurological deficit scores in all groups (n=10). D. Representative images of TTC-stained brain sections from the Sham-operated or GP17-treated animals collected 24 h after infarction; Red tissue is healthy; white tissue is infarcted. E. Quantitative analysis of the infarct volume (n=3-5). F. Rat weight in all groups (n = 6-10). G. Representative images (X400) of H/E staining performed in cortex and hippocampus CA1, CA3 regions from ischemic brains. H and I. Quantitative analysis of pathological grading scores (n=3). Mean values ± SD; $^{*}P<0.05$, $^{**}P<0.01$ versus MCAO/R group; $^{\#}P<0.05$, $^{\#\#}P<0.01$ versus Sham group, scale bar=100 μm.

GP17 protects against CIRI by regulating mitochondrial autophagy in vivo

To investigate the regulatory effect of mitochondrial autophagy in an acute model of ischemia, RAP, an autophagy inducer, and 3-MA, an autophagy inhibitor, were administered i.p. 7 days before ischemia. Interestingly, both RAP (200 μM) and 3-MA (2 mM) significantly reduced the infarct volume (Figure 2A, B) and neurological deficit scores (Figure 2C, D). Furthermore, the effect of GP17 was stronger than that of 3-MA and RAP on the infarct volume and neurological deficit scores.

To further assess whether the protective mechanism of GP17 is related to the regulation of mitochondrial autophagy, we used western blotting to analyze the

151 expression changes in autophagy signaling pathway-related proteins. Our western blot
152 results confirmed that GP17, RAP and/or 3-MA increased Beclin1 and LC3-B
153 expression and inhibited P62 expression in hippocampal and/or cortical tissues
154 (Figure 2E-I). These data suggest that inhibiting excessive levels of autophagy and
155 maintaining an appropriate level of autophagy are beneficial to improving brain injury
156 and that GP17 may play a partial protective role through autophagy.

157 In addition, compared with the OGD/R+GP17 model group, the apoptosis level
158 of the 3-MA inhibitor group was decreased, indicating that autophagy activation in the
159 acute phase of ischemia and hypoxia can partially reduce the apoptosis caused by
160 ischemia, and the RAP inducer group showed further inhibition of neuronal cell
161 apoptosis compared with that of the OGD/R group (Figure S1F), suggesting that
162 GP17 may exert a protective effect on ischemic neuronal cells in part through
163 mitochondrial autophagy regulation.

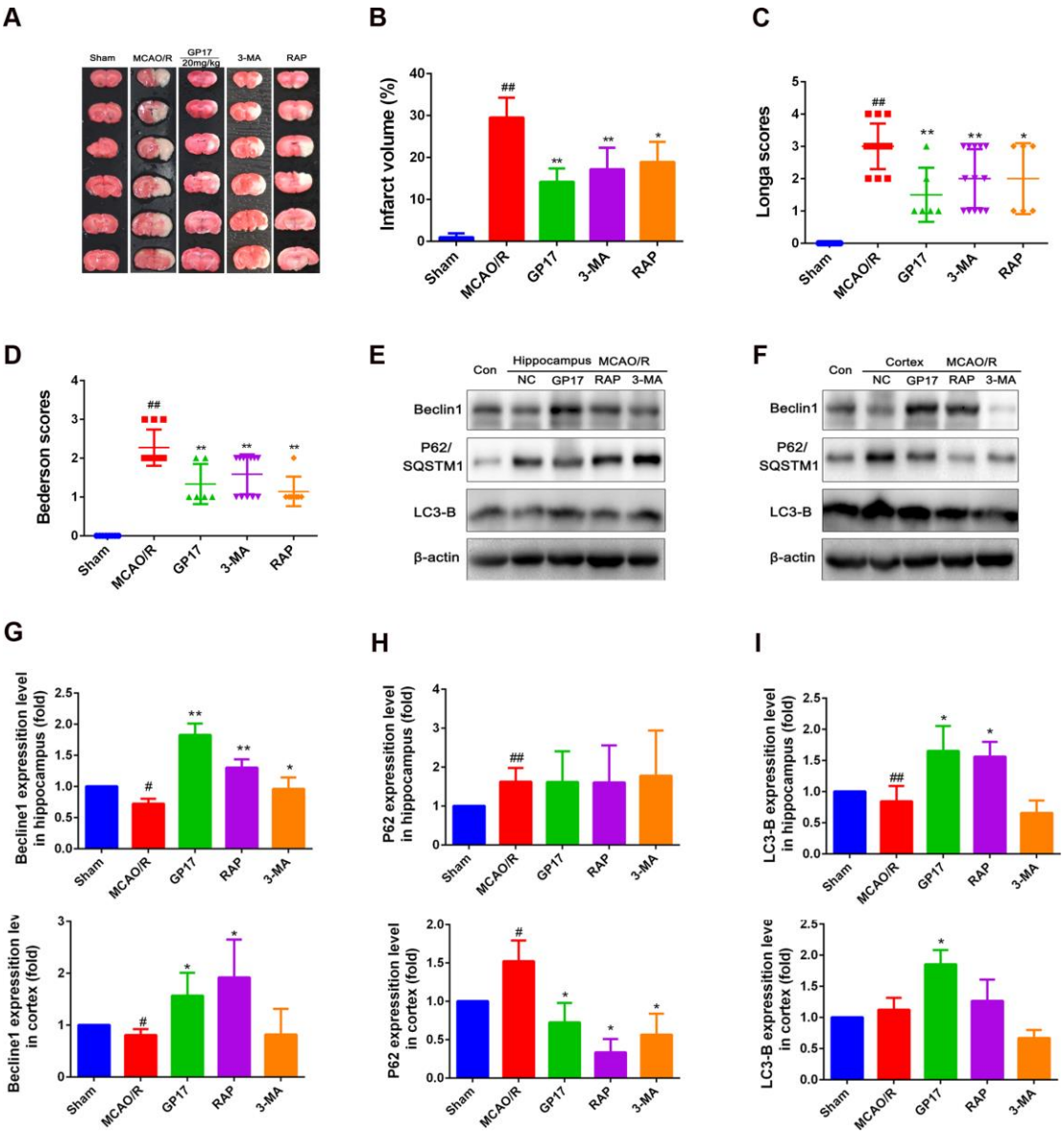

Fig. 2. Effects of GP17, autophagy activator Rapamycin (RAP) and autophagy inhibitor 3-MA on infarct volume, neurological deficit scores and Becline1-LC3-P62 signaling pathway in MCAO/R injury rats. A. Representative images of TTC-stained brain sections from the Sham-operated or GP17-treated animals collected 24 h after infarction; Red tissue is healthy; white tissue is infarcted (n = 3-6). B. Quantitative analysis of the infarct volume (n = 3). C and D. Neurological deficit scores in all

groups (n = 6-12). E and F. The protein bands of LC3-B, Becline1, and P62 in the ischemic brain sections examined by western blot analysis. G-I. The relative expression levels of LC3, Becline1, and P62, respectively, quantified and analyzed by using Gel-Pro analyzer software (n=3-6). Mean values ± SD; $^{*}P<0.05$, $^{**}P<0.01$ versus MCAO/R group; $^{\#}P<0.05$, $^{\#\#}P<0.01$, versus Sham group.

GP17 regulates mitochondrial autophagy in rats after ischemia through activation of the Hif1α-BNIP3 and SIRT1/2-FOXO3A signaling pathways

Hypoxia-induced autophagy blocks the neuroapoptosis pathway induced by mitochondrial injury through the Hif1α/BNIP3 signaling pathway[17, 18]. We wondered if Hif1α and BNIP3 participated in the mechanisms underlying the regulation of autophagy by GP17. Western blot analysis revealed that GP17 pretreatment significantly increased Hif1α and BNIP3 expression in hippocampal and/or cortical tissues compared with expression in MCAO/R rats. Furthermore, RAP pretreatment activated Hif1α in the cortex and BNIP3 in the hippocampus. There were no notable differences in Hif1α and BNIP3 in the hippocampus and cortex regions after 3-MA intervention compared with MCAO/R rats (Figure 3A-D).

Our previous study reported that the NAMPT-SIRT pathway could increase neuronal ischemic tolerance, inhibit neuronal apoptosis and necrosis, and improve

energy metabolism under ischemia [11, 12]. In this study, we found that SIRT1/2/3 expression in the hippocampus and/or cortex was markedly activated by ischemia compared with that in sham rats, but the expression of SIRT1/2 was significantly reversed by GP17 pretreatment after ischemia (Figure 3E-F, I-K).

To further explore the effect of GP17 on the downstream proteins regulated by NAMPT-SIRT1/2, we detected the expression of NAMPT, FOXO3A and MnSOD and explored the regulatory effect of GP17 on FOXO3A. We found that rats treated with GP17 exhibited significantly higher expression of NAMPT, MnSOD and FOXO3A than those treated with vehicle in the hippocampus and/or cortex regions (Figure 3G-H, L-N), implying that GP17 possibly activated the expression of the downstream protein SIRT1/2 through NAMPT, increased FOXO3A, upregulated MnSOD expression, inhibited mitochondrial oxidative damage, improved energy metabolism, and thereby inhibited neurological damages caused by ischemia.

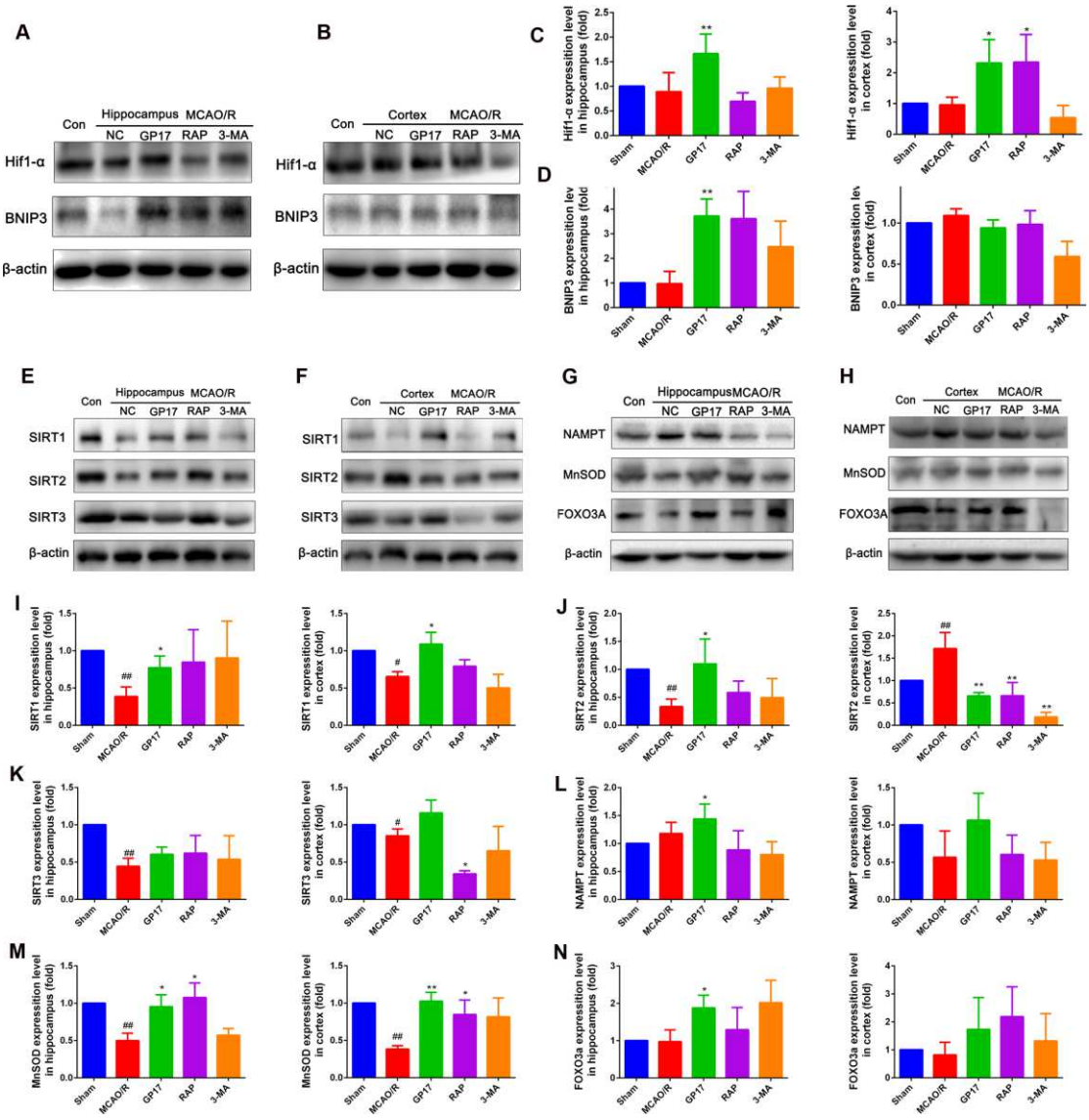

Fig. 3. Effects of GP17 on the Hif1α-BNIP3 and SIRT1/2-FOXO3A signaling pathway in MCAO/R injury rats, thus regulating mitochondrial autophagy-signaling pathway. A and B. The protein bands of Hif1α-BNIP3 in the ischemic brain sections examined by western blot analysis. C and D. The relative expression levels of Hif1α and BNIP3, respectively, quantified and analyzed by using Gel-Pro analyzer software. E and F. The protein bands of SIRT1/2/3 in the ischemic brain sections examined by western blot analysis. G and H. The protein bands of NAMPT, FOXO3A, and

MnSOD in the ischemic brain sections examined by western blot analysis. I-K. The relative expression levels of SIRT1, SIRT2 and SIRT3, respectively, quantified and analyzed by using Gel-Pro analyzer software. L-N. The relative expression levels of NAMPT, FOXO3A, and MnSOD, respectively, quantified and analyzed by using Gel-Pro analyzer software. Mean values ± SD (n=3-6); $^{*}P<0.05$, $^{**}P<0.01$, versus MCAO/R group; $^{\#}P<0.05$, $^{\#\#}P<0.01$ versus Sham group.

GP17 attenuates OGD/R-induced SH-SY5Y cell damage by regulating mitochondrial autophagy in vitro

To better characterize the effect of GP17 on mitochondrial autophagy regulation and the possible mechanism involved, we first detected autophagic vesicles in OGD/R-induced SH-SY5Y cells in vitro. GP17 notably increased the number and fluorescence intensity of acidic autophagic vesicles induced by OGD/R. To explore whether autophagy was involved in the effect of GP17 on OGD/R-induced SH-SY5Y cell damage. RAP and 3-MA were used to treat OGD/R-induced SH-SY5Y cells with the addition of GP17. The results showed that RAP pretreatment further increased the number and fluorescence intensity of acidic autophagic vesicles, while 3-MA almost completely inhibited the number and fluorescence intensity of acidic autophagic vesicles enhanced by GP17 (Figure 4A). To examine autophagic lysosomes in vitro,

we incubated GP17 with OGD/R-induced SH-SY5Y cells and examined autophagic lysosomes by immunostaining with Lyso-Tracker Red and MitoTracker Green. As shown in Figure 4B, GP17 notably increased autophagy in OGD/R-induced SH-SY5Y cells. Mitophagosome formation was also evaluated by the colocalization of the autophagy marker LC3-B (green) and the mitochondria marker MitoTracker Red. As shown in Figure 4C, mitochondrial autophagy was notably increased in GP17-treated cells, as indicated by the increased colocalization of GFP-LC3-B and MitoTracker Red, and RAP pretreatment more strongly increased mitochondrial autophagy than GP17. In addition, mitochondrial autophagy was significantly decreased in GP17-treated cells with 3-MA pretreatment. These results suggest that GP17 activates mitochondrial autophagy in OGD/R-induced SH-SY5Y cells.

We continued to examine the expression of the major mitochondrial autophagy signaling pathway-related proteins in SH-SY5Y cells. We found that GP17 increased LC3-B and Beclin1 expression and inhibited p62 expression in OGD/R-induced SH-SY5Y cells. All the upregulated protein expression was further facilitated by RAP, except that RAP did not significantly affect the expression of p62 (Figure 4D-G).

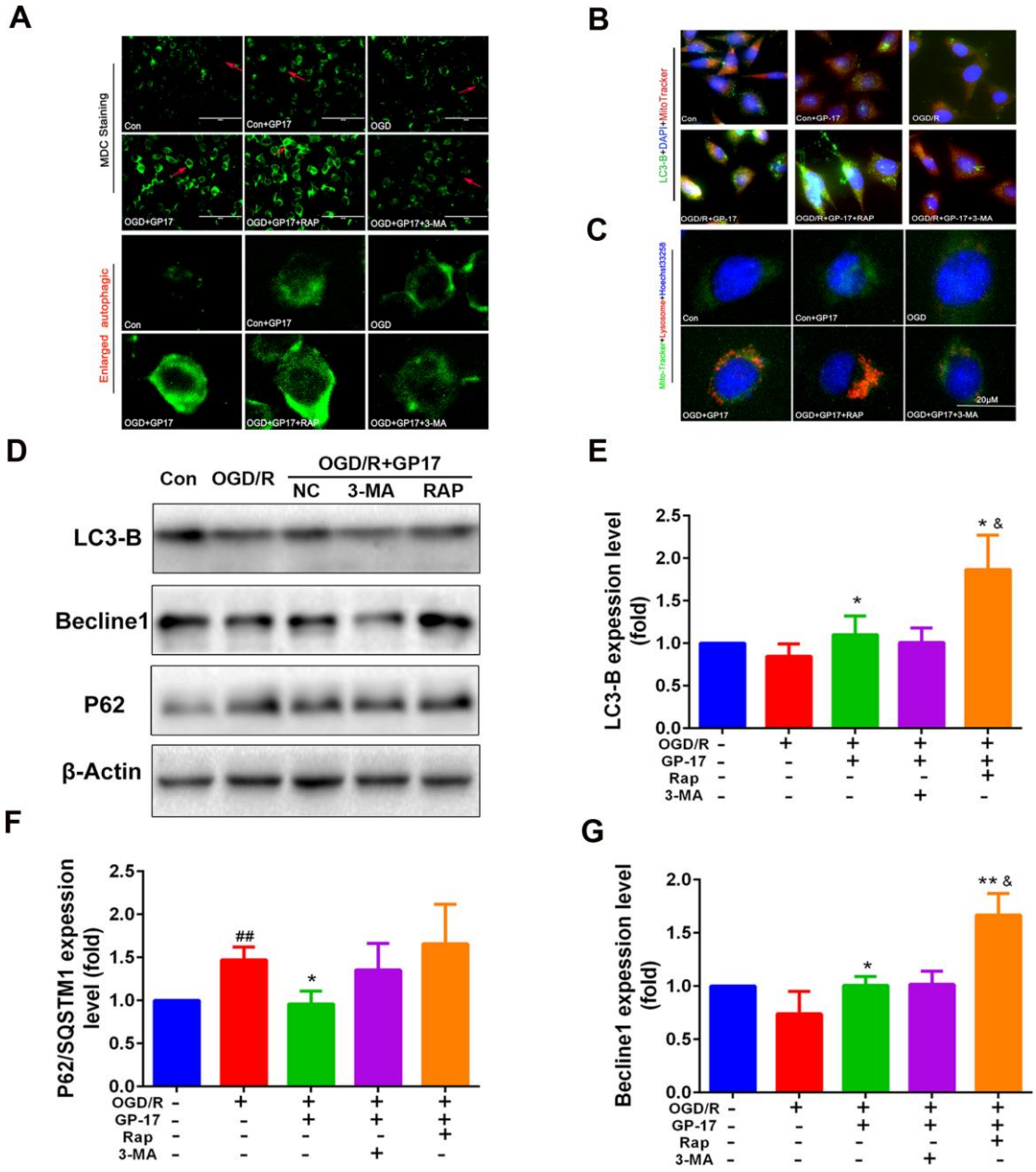

Fig. 4. Effects of GP17 on autophagy vesicles, autophagy lysosome, LC3-B expression and Becline1-LC3-P62 signaling pathway in OGD/R-induced SH-SY5Y cells, partly reversed by the inhibitor 3-MA. A. The MDC staining images from all SH-SY5Y cell groups, measured by a fluorescence microscope, scale bar=100 μm. B. The triple staining of autophagy-lysosome (Red)、mitochondria (Green) with the nucleus (Blue) in the OGD/R-induced SH-SY5Y cells, measured by a fluorescence

microscope, scale bar=20 μm. C. The triple staining of LC3-B protein (Green)、mitochondria (Red) with the nucleus (Blue) in the OGD/R-induced SH-SY5Y cells, respectively, located and measured by a fluorescence microscope, scale bar, 20 μm. D. The protein bands of LC3-B, Becline1 and P62, respectively, were examined by western blot analysis in the OGD/R-induced SH-SY5Y cells. E-G. The relative expression levels of LC3-B, Becline1 and P62, were quantified and analyzed by using Gel-Pro analyzer software in the OGD/R-induced SH-SY5Y cells. The data presented as Mean values ± SD (n-3-6). $^{\#}P < 0.05$, $^{\#\#}P < 0.01$ versus the control group; $^{*}P < 0.05$, $^{**}P < 0.01$ versus the OGD/R model group; $^{\&}P < 0.05$, $^{\&\&}P < 0.01$ versus the OGD/R+GP17 group.

SIRT1/2 and Hif1α inhibition abolishes the effect of GP17 on mitochondrial autophagy-related indicators in OGD/R-induced SH-SY5Y cells

To assess whether the SIRT1/2 and/or Hif1α signaling pathways were associated with the mitochondrial autophagy-related indicators of GP17, the SIRT1/2/3 inhibitor AGK-7 and the Hif1α inhibitor 2-ME were used to treat SH-SY5Y cells along with GP17. First, we investigated the viability of normal SH-SY5Y cells treated with AGK-7 (0.1, 0.5, 1.0, 5.0 and 10 μM) and 2-ME (1.0, 5.0, 10.0 and 20.0 μM). As shown in Figure S2A and B, AGK-7 incubation at 0.5-10 μM significantly inhibited

269 the viability of SH-SY5Y cells compared with that of the control treatment. 2-ME
270 incubation at 10.0 and 20.0 μM significantly inhibited the viability of SH-SY5Y cells
271 compared with that of the control treatment. We selected 0.1 μM AGK-7 and 2.5 μM
272 2-ME to further verify the molecular mechanism by which GP17 regulates
273 mitochondrial autophagy.

274 We next evaluated the MMP and viability in SH-SY5Y cells upon challenge with
275 OGD/R induction, GP17 or AGK-7 and 2-ME. Figure 5A and B shows that either
276 AGK-7 or 2-ME decreased the MMP and mitochondrial viability in GP17- and
277 OGD/R-cotreated SH-SY5Y cells. To determine the effect of GP17 on mitochondrial
278 function, we evaluated oxidative phosphorylation and glycolysis by measuring the
279 oxygen consumption rate (OCR) and extracellular acidification rate (ECAR),
280 respectively, in a seahorse assay. Figure S3A-D shows that the OCR and ECAR in the
281 GP17 and OGD/R cotreated group were significantly higher than those in the OGD/R
282 group. However, AGK-7 and 2-ME abolished the beneficial effect of GP17 on
283 mitochondrial function in OGD/R-induced SH-SY5Y cells.

284 To further assess whether the SIRT1/2 and/or Hif1α signaling pathways were
285 involved in the regulation of mitochondrial autophagy by GP17, AGK-7 and 2-ME
286 were used to treat SH-SY5Y cells along with GP17. Figure 5D shows that both

AGK-7 and 2-ME significantly inhibited the colocalization of GFP-LC3-B and MitoTracker Red enhanced by GP17. The western blot results also confirmed that AGK-7 and/or 2-ME decreased LC3-B, Beclin1 and p62 expression in the GP17 and OGD/R cotreated group (Figure 5E-G). These data suggested that GP17 can ameliorate ischemia/hypoxia-induced neuronal injury by regulating mitochondrial autophagy, and this effect is closely related to the SIRT1/2 and Hif1α pathways.

In addition, GP17 incubation for 24 h significantly reduced OGD/R-induced apoptosis. However, AGK-7 and 2-ME treatment reduced the inhibitory effect of GP17 on apoptosis compared with that of the OGD/R+GP17 group, suggesting that the reduction in ischemia-induced apoptosis by GP17 may be through NAMPT-regulated downstream SIRT1/2 and the Hif1α pathway, and the results are consistent with the in vivo results (Figure S2C).

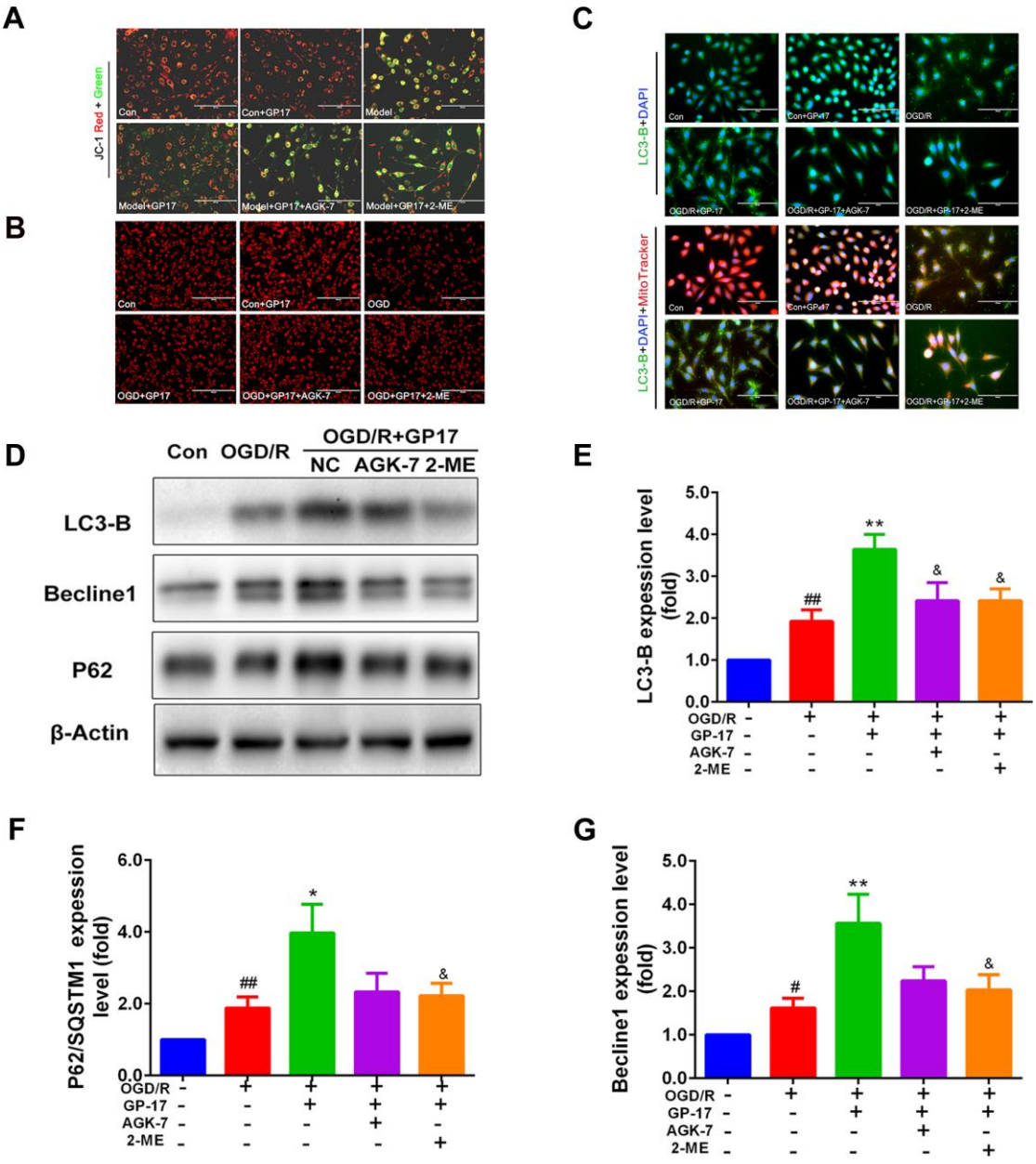

299

300 **Fig. 5.** Effects of GP17 on mitochondrial related indicators and autophagy

301 Becline1-LC3-P62 signaling pathway in OGD-induced SH-SY5Y cells, which partly

302 reversed by the inhibitors AGK-7 and 2-ME. A. The mitochondria fluorescence

303 images of GP17 on the mitochondrial membrane potential (MMP) in OGD/R-induced

304 SH-SY5Y cells, measured with the JC-1 assay by a fluorescence microscope, scale

305 bar, 100 μm. B. The representative images of mitochondria, stained by the

MitoTracker-Red-CMXRos, measured by a fluorescence microscope, scale bar, 200 μm. C. The triple staining of LC3-B protein (Green)、mitochondria (Red) with the nucleus (Blue) in the OGD/R-induced SH-SY5Y cells, repectively, located and measured by a fluorescence microscope, scale bar=20 μm. D. The protein bands of LC3, Becline1 and P62, respectively, were examined by western blot analysis in the OGD/R-induced SH-SY5Y cells. E-G. the relative expression levels of LC3, Becline1 and P62, were quantified and analyzed by using Gel-Pro analyzer software in the OGD/R-induced SH-SY5Y cells. The data presented as Mean values ± SD (n=3). $^{\#}P < 0.05$, $^{\#\#}P < 0.01$ versus the control group; $^{*}P < 0.05$, $^{**}P < 0.01$ versus the OGD/R model group; $^{\&}P < 0.05$, $^{\&\&}P < 0.01$ versus the OGD/R+GP17 group.

SIRT1/2 and Hif1α inhibition abolishes the effect of GP17 on the Hif1α-BNIP3 and SIRT1/2-FOXO3A signaling pathways in OGD/R-induced SH-SY5Y cells

GP17 regulates mitochondrial autophagy through activation of the Hif1α and/or SIRT1/2 signaling pathways. The regulation of the Hif1α-BNIP3 and SIRT1/2-FOXO3A pathways by GP17 was explored using immunofluorescence and western blotting, and the potential mechanism was verified by the inhibitors AGK-7 and 2-ME. Immunofluorescence analysis revealed that GP17 significantly increased BNIP3 expression in OGD/R-induced SH-SY5Y cells compared with that in the

OGD/R group. However, AGK-7 and 2-ME pretreatment reversed BNIP3 expression (Figure 6A-B). Similarly, both AGK-7 and 2-ME significantly inhibited Hif1α and BNIP3 protein expression induced by GP17 (Figure 6C-E).

In an *in vivo* study, we found that GP17 pretreatment markedly increased SIRT1/2/3 expression in the hippocampus and/or cortex regions compared with that in MCAO/R rats. Here, we also found that GP17 markedly increased SIRT1/2/3 and MnSOD expression in OGD/R-induced SH-SY5Y cells compared with that in the OGD/R group. AGK-7 significantly inhibited the increase in the expression of these proteins induced by GP17 (Figure 6F-J). Notably, the trend of SIRT1/3 but not SIRT2 being inhibited is obvious with 2-ME treatment. Combined with in vivo experiments, these findings indicated that GP17 can regulate the mitochondrial autophagy-related Hif1α-BNIP3 pathway through NAMPT-SIRT1, exerting a neuroprotective effect in the process of hypoxia-ischemia.

To further determine the relationship between the regulation of FOXO3A by GP17 and the SIRT1/Hif1α/BNIP3 pathway, we detected the expression of FOXO3A in vitro using immunofluorescence and western blotting upon stimulation with GP17, AGK-7 and 2-ME. Figure 6K and L shows that cells treated with GP17 exhibited a significantly lower fluorescence intensity of FOXO3A than those treated with vehicle.

However, the trend of decreased FOXO3A fluorescence after 2-ME treatment was reversed. The western blot results showed that both AGK-7 and 2-ME increased FOXO3A protein expression that had been reduced by GP17, indicating that Hif1α and FOXO3A jointly participate in the downstream processes mediated by SIRT1 (Figure 6M, N).

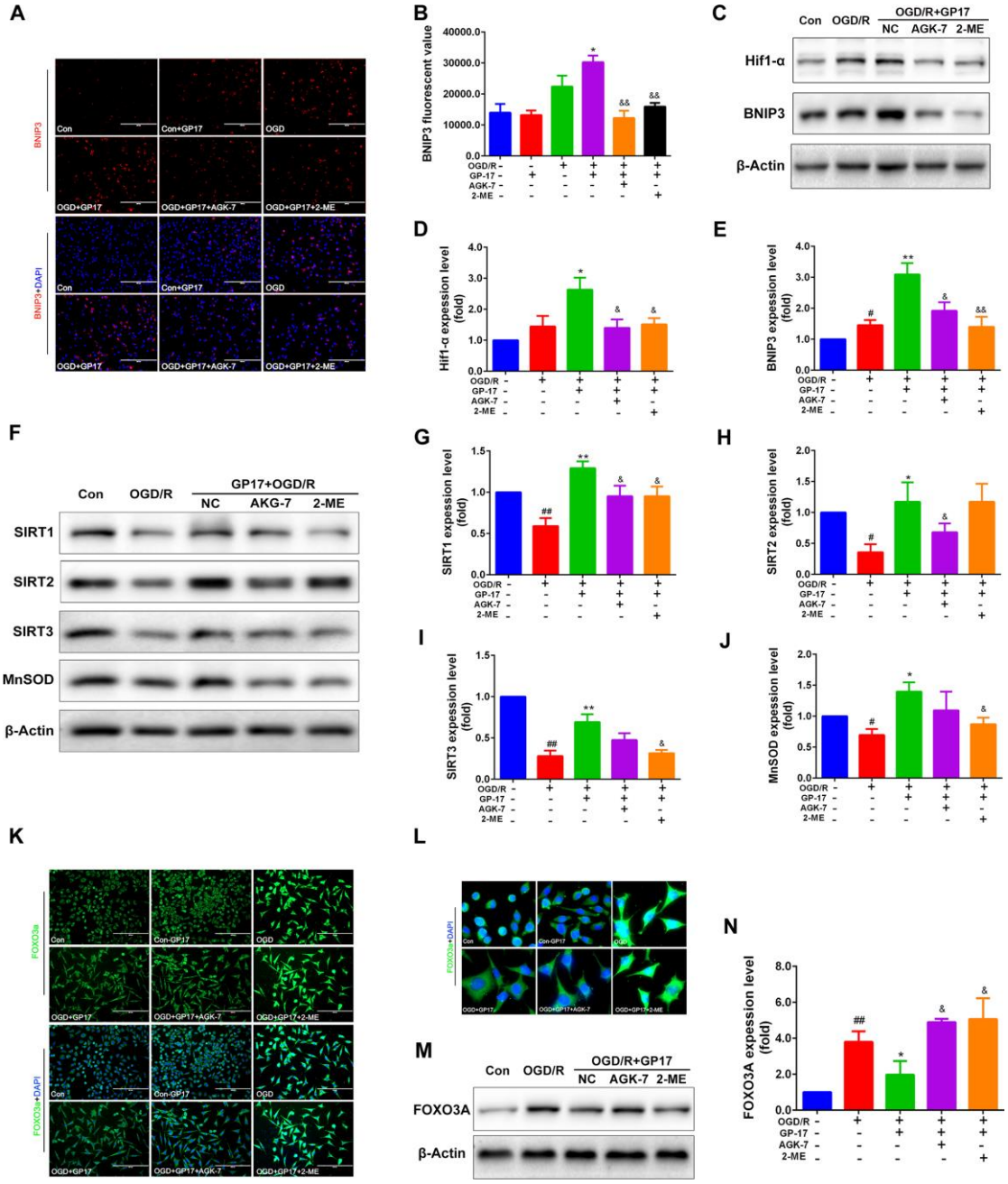

Fig. 6. Effects of GP17 on the Hif1α-BNIP3 and SIRT1/2/3-FOXO3A signaling pathway in the OGD/R-induced SH-SY5Y cells, which partly reversed by the inhibitors AGK-7 and 2-ME. A. The double staining of the BNIP3 protein (Red) with the nucleus (Blue) in the OGD/R-induced SH-SY5Y cells, respectively, located and measured by a fluorescence microscope, scale bar=200 μm. B. The statistical data analysis of BNIP3 fluorescence via the Image J software. C. The protein bands of Hif-1α and BNIP3 were examined by western blot analysis in the OGD/R-induced SH-SY5Y cells. D and E. The relative expression levels of Hif-1α and BNIP3 were quantified and analyzed by using Gel-Pro analyzer software in the OGD/R-induced SH-SY5Y cells. The data presented as Mean values ± SD (n=3-6). F. The protein bands of SIRT1/2/3 and MnSOD were examined by western blot analysis in the OGD/R-induced SH-SY5Y cells. G-J. The relative expression levels of SIRT1/2/3 and MnSOD were quantified and analyzed by using Gel-Pro analyzer software in the OGD/R-induced SH-SY5Y cells. The data presented as Mean values ± SD (n=3). K. The double staining of the FOXO3A protein (green) with the nucleus (Blue) in the OGD/R-induced SH-SY5Y cells, respectively, located and measured by a fluorescence microscope, scale bar=100 μm. L. The FOXO3A protein images enlarged. M. The relative expression levels of FOXO3A were quantified and analyzed

by using Gel-Pro analyzer software in the OGD/R-induced SH-SY5Y cells. N. The protein bands of FOXO3A were examined by western blot analysis in the OGD/R-induced SH-SY5Y cells. The data presented as Mean values ± SD (n=3). $^{\#}P < 0.05$, $^{\#\#}P < 0.01$ versus the control group; $^{*}P < 0.05$, $^{**}P < 0.01$ versus the OGD/R model group; $^{\&}P < 0.05$, $^{\&\&}P < 0.01$ versus the OGD/R+GP17 group.

Discussion

GP17 is a dammarane-type 20-(S)-protopanaxadiol-type saponin that mainly exists in the stems and leaves of Panax notoginseng and Gynostemma pentaphyllum and has significant pharmacological activity [19]. Our previous research found that GP17 can significantly inhibit brain cognitive damage and improve MPTP- and glutamate-induced neuronal oxidative damage, indicating that GP17 has neuroprotective effects [15, 16]. In this study, we first conducted in vivo experiments and found that GP17 administration could significantly improve neurological function damage induced by MCAO/R, inhibit cerebral infarction volume, alleviate the pathological changes in brain tissue caused by ischemia, and inhibit oxidative damage and inflammatory responses during acute cerebral ischemia. However, the molecular mechanisms of the neuroprotective effect of GP17 on ischemic brain injury and the inhibition of mitochondrial damage are still unclear.

In the process of cerebral ischemia, the regulation of mitochondrial autophagy can reduce neuronal apoptosis induced by cerebral infarction and produce neuroprotective effects [6]. In this study, we found that GP17 administration regulated the expression of Beclin1-LC3-P62 protein in ischemic brain regions to varying degrees in the MCAO/R rat model, consistent with that in the autophagy inducer RAP group. After using the OGD/R cell model, we found that the labeled autophagic vacuoles, autophagic fluorescent spots and autophagic lysosomes in the cells were significantly increased after GP17 treatment; the expression of the intracellular Beclin1-LC3-P62 protein was activated; and the above changes were reversed by the inhibitor 3-MA. These results are consistent with relevant reports [14, 15, 20]. These in vitro and in vivo results suggest that GP17 could regulate mitochondrial autophagy. However, compared with cotreatment with GP17 and RAP, excessive activation of autophagy did not increase the inhibitory effect on apoptosis. Combined with the results of rat experiments in vivo, both the inhibitor and inducer groups showed partial protective effects, which suggested that maintaining appropriate levels of autophagy and inhibiting excessive levels of autophagy in the acute phase of ischemia may alleviate early ischemic brain damages.

Hif1α is a hypoxia-inducing factor that plays a key role in tissue adaptation to

ischemia/hypoxia [17, 21], but under prolonged hypoxic conditions, Hif1α overexpression regulates mitochondrial respiration, resulting in increased levels of ROS and apoptosis [22-24]. BNIP3 is a mitochondrial outer membrane protein with very low levels of expression under normal physiological conditions, and in hypoxic environments, activated Hif1α upregulates the expression of BNIP3, causing Beclin1 to dissociate from Bcl-XL and Bcl-2 and thereby releasing Beclin1 [6, 18]. Beclin1 can promote mitochondrial autophagy by triggering E3 ubiquitin ligase Parkin translocation to mitochondria or by directly binding to LC3-B on autophagosomes [6]. Recent studies have found that autophagy activation can be mediated through the Hif1α/BNIP3 pathway. Selective activation of appropriate levels of mitochondrial autophagy clears damaged mitochondria, blocks the release of CytC and the activation of Caspase-9/Caspase-3, stabilizes MMP, and increases the ratio of Bcl-2/Bax to block the apoptosis pathway induced by mitochondrial injury, thereby protecting against cerebral ischemic neuron damage [6, 25]. Our findings are consistent with related reports that MCAO/R induces the upregulation of Hif1α and BNIP3, suggesting that GP17 may regulate the Hif1α-BNIP3 pathway to mediate autophagy in the acute phase of cerebral ischemia. To verify the above experimental results, we treated OGD/R-induced SH-SY5Y cells with 2-ME, a specific inhibitor of Hif1α, and found

that GP17 treatment activated the Hif1α-BNIP3 pathway, but 2-ME treatment blocked the upregulation of Hif1α, and the transcriptional expression level of BNIP3 was also reduced.

The SIRTUIN protein family is a class of NAD^+-dependent protein deacetylases and ADP ribosyltransferases with a highly conserved core region [26-28]. The mammalian SIRT protein family can interact with p53, FOXO, PGC-1α, NF-κB, Ku70 and other proteins to regulate the cellular stress response, thereby affecting biological processes such as cell metabolism, aging and apoptosis [26, 27, 29]. GP17 is an important active substance in PNGL. In vivo, we found that GP17 regulates the downstream protein SIRT1/2/3 level of NAMPT, mainly SIRT1; activates transcription factors related to antioxidant and inflammatory responses; and improves nerve resistance to ischemia. This finding suggests that GP17 can induce the expression of NAMPT, regulate NAMPT-mediated downstream pathways, and improve neuron viability.

To further explore the regulation of the SIRT1/2/3 pathway by GP17, we used the specific inhibitor AGK-7 to study the SH-SY5Y cell model subjected to OGD/R. The results showed that the expression of SIRT1/2/3 induced by OGD/R decreased, while GP17 treatment significantly increased the expression levels of the proteins

SIRT1, SIRT2 and SIRT3. However, treatment with the inhibitor AGK-7 significantly reversed the changes in expression of SIRT1 and SIRT3, and the changes in the expression of SIRT1 were more significant. The comprehensive in vitro and in vivo results suggest that the protective effect of GP17 in the process of hypoxia-ischemia may be mainly related to the regulation of SIRT1. At the same time, it was found that the inhibitor AGK-7 partially reversed the upregulation of Hif1α by GP17. Combined with related reports, it was suggested that SIRT1, upstream of Hif1α, and BNIP3 were involved in the regulation of mitochondrial autophagy under ischemia.

In addition, treatment with the inhibitors AGK-7 and 2-ME blocked the regulation by GP17 of the SIRT1/2/3 and Hif1α-BNIP3 molecular pathways, and the regulation of autophagy spots, Beclin1, and LC3-B expression by GP17 was significantly reversed by the inhibitor 2-ME and partially reversed by the inhibitor AGK-7. As autophagy and mitochondrial regulation were reversed, we found that the neuroprotective effect of GP17 was partially blocked. These results indicate that GP17 can alleviate ischemic injury, reduce mitochondrial dysfunction, increase the number of mitochondria, and improve mitochondrial viability. This protective effect is achieved through mitochondrial autophagy mediated by the SIRT1/2/3 and Hif1α-BNIP3 pathways.

FOXO3A is a human protein encoded by the FoxO3 gene, and its family includes FoxO1, FoxO3, FoxO4 and FoxO6. Recent research has shown that FOXO3A can regulate cell differentiation and proliferation, improve metabolism, inhibit apoptosis, repair damaged DNA, and regulate oxidative stress through the PI3K-AKT-FOXO3A, SIRT1-FOXO3A, AMPK-FOXO3A-MnSOD and other pathways [30-34]. In a previous study, we found that PNGL has a protective effect through the SIRT1-FOXO3A pathway, and this study found that GP17 can regulate FOXO3A acetylation in the cytoplasm through SIRT1/2 in in vivo and in vitro models, increase the binding of FOXO3A to DNA, and enhance the expression of FOXO3A target genes and promote cell survival, which may be the common molecular mechanism of PNGL components against ischemic injury. At the same time, intracellular MnSOD protein expression was significantly increased after GP17 treatment, and MnSOD expression was reversed after treatment with the inhibitor AGK-7, indicating that SIRT1/3 is an important upstream regulatory molecule.

FOXO3A is the intersection of multiple signaling pathways in oxidative stress. FOXO3A induces autophagy by inducing the expression of autophagy-related genes, such as LC3, BNIP3, Beclin1, and Atg12, but excessive autophagy can induce cell apoptosis [30, 35, 36]. Previous studies have found that SIRT1/2/3 (mainly SIRT1)

may interact with Hif1α upstream of Hif1α during GP17 regulation of ischemic injury[37]. At the same time, we further found that GP17 treatment significantly reduced the intracellular FOXO3A level induced by OGD/R, but the downregulation of FOXO3A by GP17 was reversed by 2-ME, a specific inhibitor of Hif1α, suggesting that the regulation of SIRT1-FOXO3A involves the Hif1α-BNIP3 pathway, and the two regulations are opposing, implying that it could inhibit the overactivation of the Hif1α-BNIP3 pathway induced by ischemia and hypoxia, allowing the two to participate in the downstream autophagy process.

Taken together, this study confirmed the preventive and therapeutic effects of GP17 on ischemic stroke and explored and analyzed the effect and molecular mechanism by which GP17 inhibits mitochondrial damage and inhibits ischemia-induced neuroapoptosis. The mechanism is partly through SIRT1-FOXO3A/Hif1a-BNIP3-mediated mitochondrial autophagy, which regulates the downstream signaling pathways of PGC-1α, SOD1, and SOD2; inhibits mitochondrial damage; alleviates oxidative stress and apoptosis induced by ischemia and hypoxia; improves neuroviability; and has a preventive effect on ischemic stroke (Figure 7). Therefore, this study elucidates the effect and molecular mechanism of GP17 in ameliorating ischemic injury and shows that GP17 is a promising compound

that provides great potential for development of new therapeutic agents for ischemic stroke.

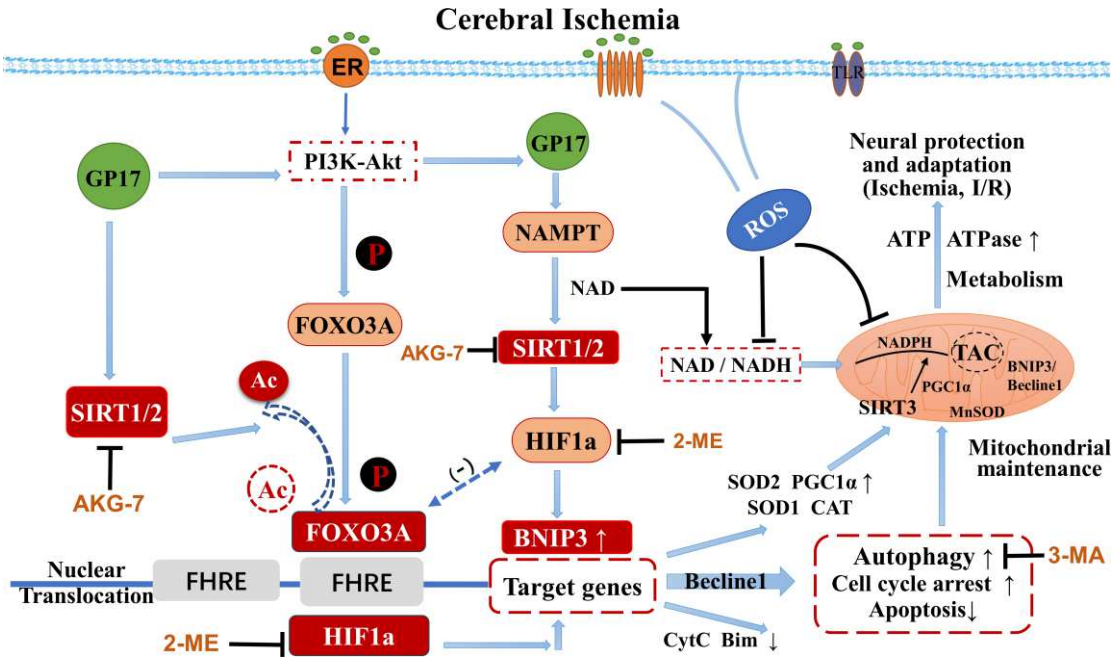

Fig. 7. Effects and mechanisms of GP17 against cerebral ischemic injury via the mitochondrial autophagy regulation mediated by the SIRT1/2/3-FOXO3A/Hif1a-BNIP3 signal pathways, thus inhibiting mitochondrial damage, improving energy metabolism, and alleviating neural apoptosis.

Materials and methods

Materials

GP17 (molecular weight = 947.154; purity > 98%) was purchased from Beijing Beina Chuanglian Biotechnology Research Institute (Beijing, China). The positive control drug dl-3-n-butylphthalide (NBP) was obtained from CSPC NBP Pharmaceutical Co., Ltd. Triphenyltetrazolium chloride (TTC) was purchased from Sigma–Aldrich (MO,

United States). The primary antibodies against p62/SQSTM1, LC3-B, BNIP3, NAMPT, SIRT1, SIRT2, MnSOD, PGC-1α, FOXO3 and p-FOXO3 were provided by Abcam (Cambridge, UK). The primary antibodies against Hif1α and Beclin1 were provided by Proteintech (Wuhan, China). The primary antibody against SIRT3 was provided by Cell Signaling Technology (MA, USA). The RAP inducer and 3-MA and 2-ME inhibitors were obtained from MedChemExpress (New Jersey, USA). The AGK-7 inhibitor was obtained from Abcam (Cambridge, UK). The ELISA kits for IL-6, TNF–α, MCP-1, T-AOC and 4-HNE were acquired from HaiTai TongDa Sci Tech Ltd. (Beijing, China).

Animals

Male Sprague–Dawley (SD) rats (obtained from Beijing Vital Lihua Experimental Animals Co., Ltd.) (weighing 220~240 g) were used in this study. All operations and treatments were required to conform to the Declaration of Helsinki and the "3R" principles. The experimental protocol was approved in accordance with the Laboratory Animal Ethics Committee (Permit Number: SYXK 2017-0020). All rats were housed in ventilated cages with a 12-hour light/dark cycle, at 20~25°C in a temperature-controlled room with free access to food and water.

MCAO surgery

The SD rats were anesthetized with Zoletil 50 (10~15 mg/kg) intraperitoneally (i.p.) and subjected to the MCAO procedure. A rat model of Cerebral I/R was operated on using the suture occlusion technique described in our previous study[38]. The sham-operated rats underwent the same procedure, the difference being that the sutures were not inserted into the internal carotid artery. The body temperature was maintained at 37 ± 0.5°C using a heat pad (Sunbeam, United States). The grouping of animals was conducted as a blinded experiment, and the researchers did not know which group each of the animals were assigned to.

Drug treatment

The drug was dissolved in 0.9% normal saline prior to administration. The drug was administered by intraperitoneal (i.p.) injection. To select the drug dosages, GP17 (10 mg/kg and 20 mg/kg) and NBP (positive control drug, 20 mg/kg) were administered for 7 days before MCAO surgery. To detect mitochondrial autophagy, rats were divided into 5 groups: the sham group, the MCAO/R group, the GP17 (20 mg/kg) + MCAO/R group, the RAP (2 mg/kg) + MCAO/R group and the 3-MA (3 mg/kg) + MCAO/R group. The sham and MCAO/R groups were given 0.9% normal saline solution i.p. daily.

Neurological score

Neurological behavior was investigated at 24 h after I/R by two blinded investigators using Zea Longa scores [39, 40] and Bederson scores [41], as previously published. Higher scores represent more severe neurological deficits.

TTC staining

TTC staining was conducted 24 h after I/R to determine the infarct volume and was performed as previously described methods [10]. 2-mm coronal slices were obtained to calculate infarct volume. Brain slices were stained with 2% TTC at 37°C for 20 min and fixed overnight in 4% paraformaldehyde. The cerebral infarct area on each slice was quantified by using ImageJ 1.44p software (National Institutes of Health, Bethesda, MD, USA).

H&E staining

H&E staining was performed according to previously described methods [10, 42]. Intact brains were prepared, and pathological paraffin sections (5-μm thick) were made. The staining images were acquired using a pathological scanner and analysis system (Aperio CS2, Leica, Wetzlar, Germany).

Oxygen-glucose deprivation/reoxygenation and drug treatment

OGD/R method was described according to our previous study [39]. Briefly, SH-SY5Y cells were cultured in glucose-free Locke's medium, played in the

559 anaerobic chamber (TYPE c; Coy Laboratory Products, Inc., Grasslake, MI, United
560 States) for 4 h. Then, the cells were removed from the anaerobic chamber to a
561 normoxic environment, the medium was returned to normal medium for 24 h. In the
562 GP17-treated group, SH-SY5Y cells subjected to ODG/R were pretreated with GP17
563 (6.25 μM) for 24 h. In the inhibitor-treated group, the cells were preincubated with
564 100 nM AGK-7 and 1.0 μM 2-ME for 1 h prior to treatment with GP17.

565 **Determination of MMP**

566 Mitochondrial membrane potential (MMP) was assessed using a JC-1 MMP assay kit
567 (C2006, Beyotime, Shanghai, China) we described earlier [12]. Briefly, SH-SY5Y
568 cells were washed twice with FBS-free DMEM and then incubated with JC-1 (200
569 μM) for 20 min at 37°C, followed by washing with DMEM to remove excess JC-1.
570 The fluorescence images of JC-1 in cells observation using a fluorescence microscopy
571 (EVOS M5000, Thermo Fisher Scientific, USA). MMP was calculated by the ratio of
572 red to green fluorescence.

573 **Assessment of mitochondrial viability**

574 After incubation and treatments, mitochondrial viability was evaluated using our
575 previous method [12]. SH-SY5Y cells were washed twice with DMEM and then
576 incubated with the MitoTracker Red CMXRos probe (50 nM) for 45 min at 37°C,

577 followed by washing with DMEM. Fluorescence images of mitochondrial viability in
578 cells observation using a fluorescence microscopy (EVOS M5000, Thermo Fisher
579 Scientific, USA).

580 **Immunofluorescence staining**

581 Immunofluorescence staining was performed using our previous method [43, 44].
582 Primary antibodies against LC3-B, BNIP3 and FOXO3A were used for the
583 experiment. Images were obtained through at least three random visual fields from
584 three separate sections of each sample by using a fluorescence microscope (Carl Zeiss,
585 Germany).

586 **ELISA assay**

587 Enzyme-linked immunosorbent assay (ELISA) kits were used according to the
588 manufacturer's instructions and a previously described method [10, 45] to quantify
589 the expression of IL-6, TNF-α, MCP-1, T-AOC and 4-HNE in the serum.

590 **Western blot analysis**

591 Western blot analysis was performed according to our previously described method
592 [11, 42]. Based on the standard operating specifications, total proteins were extracted
593 with lysate and equal amounts of proteins were separated by 10% SDS
594 polyacrylamide gel electrophoresis. The proteins were transferred to nitrocellulose

membranes and the membranes were blocked before being incubated overnight at 4°C with the appropriate primary antibodies: p62/SQSTM1 (ab56416, 1:1000), LC3-B (ab48394, 1:1000), Hif1α (20960-1-AP, 1:1000), BNIP3 (ab239976, 1:1000), Beclin1 (11306-1-AP, 1:1000), NAMPT (ab236873, 1:1000), SIRT1 (ab189494, 1:1000), SIRT2 (ab211033, 1:2000), SIRT3 (cst5490, 1:1000), FOXO3A (ab109629, 1:3000), p-FOXO3A (ab52857, 1:1000), MnSOD (ab137037, 1:5000), PGC-1a (ab188102, 1:5000) and β-actin (EXP0041F, 1:3000).

Statistical analysis

Statistical program SPSS 21.0 (SPSS, IBM, Chicago, IL, USA) were used for statistical analysis. Data are expressed as the mean ± SD. When the Kruskal–Wallis H test showed a significant difference, the Mann–Whitney U test with the Bonferroni correction was used. All other data were analyzed using one-way ANOVA followed by the least significant difference (LSD) or Bonferroni's method, and $p < 0.05$ was considered statistically significant.

Supplementary Information

The online version contains supplementary material available at

Authors' contributions

XS conducted the study. WX designed the detailed experiments, performed the study, and collected and analyzed data. TZ, SZ took part in the animal experiments in this study. TZ wrote the manuscript and SZ helped to revise it. All authors discussed, edited, and approved the final version.

Finding

This work was supported by the National Natural Science Foundation of China (No. 81891012), National Natural Science Foundation of China (No. U20A20405), CAMS Innovation Fund for Medical Sciences (CIFMS) (No. 2021-I2M-1-031), and the National natural science foundation of China (No. U1812403-5-3).

Availability of data and materials

All data generated or analyzed during this study are included in this article (and its additional files).

Declarations

Ethics approval and consent to participate

All operations and treatments were required to conform to the Declaration of Helsinki and the "3R" principles. The experimental protocol was approved in accordance with the Laboratory Animal Ethics Committee (Permit Number: SYXK 2017-0020).

Consent for publication

Not applicable.

Competing interests

The authors declare no competing financial interests.

Author details

[1]Institute of Medicinal Plant Development, Peking Union Medical College and Chinese Academy of Medical Sciences, Beijing 100193, China. [2]Key Laboratory of Material Basis and Resource Utilization of Chinese Herbal Medicine, Beijing 100193, China. [3]State Administration of Traditional Chinese Medicine Key Laboratory of Efficacy evaluation of Traditional Chinese Medicine in intervention of disorders of glucose and Lipid Metabolism, Beijing 100193, China. [4]Institute of Neuroregeneration & Neurorehabilitation, Department of Pathophysiology, School of Basic Medicine, Qingdao University, Qingdao 266071, China. [5]Shanghai Mental Health Centre, School of Medicine, Shanghai Jiao Tong University, Shanghai 200011, China.

References

1. Zhang M, Ying W. NAD(+) Deficiency Is a Common Central Pathological Factor of a Number of Diseases and Aging: Mechanisms and Therapeutic Implications.

649 Antioxidants & redox signaling. 2019; 30: 890-905.

650 2. Zhao Y, Guan YF, Zhou XM, Li GQ, Li ZY, Zhou CC, et al. Regenerative
651 Neurogenesis After Ischemic Stroke Promoted by Nicotinamide
652 Phosphoribosyltransferase-Nicotinamide Adenine Dinucleotide Cascade. Stroke.
653 2015; 46: 1966-74.

654 3. Zhao Y, Liu XZ, Tian WW, Guan YF, Wang P, Miao CY. Extracellular visfatin
655 has nicotinamide phosphoribosyltransferase enzymatic activity and is
656 neuroprotective against ischemic injury. CNS neuroscience & therapeutics. 2014;
657 20: 539-47.

658 4. Yu A, Zhou R, Xia B, Dang W, Yang Z, Chen X. NAMPT maintains
659 mitochondria content via NRF2-PPARα/AMPKα pathway to promote cell
660 survival under oxidative stress. Cellular signalling. 2020; 66: 109496.

661 5. Wang N, Yang L, Zhang H, Lu X, Wang J, Cao Y, et al. MicroRNA-9a-5p
662 Alleviates Ischemia Injury After Focal Cerebral Ischemia of the Rat by Targeting
663 ATG5-Mediated Autophagy. Cellular physiology and biochemistry: international
664 journal of experimental cellular physiology, biochemistry, and pharmacology.
665 2018; 45: 78-87.

666 6. Wang P, Shao BZ, Deng Z, Chen S, Yue Z, Miao CY. Autophagy in ischemic

667 stroke. Progress in neurobiology. 2018; 163-164: 98-117.

668 7. Rubinsztein DC, Mariño G, Kroemer G. Autophagy and aging. Cell. 2011; 146:
669 682-95.

670 8. Zhu T, Wang L, Wang LP, Wan Q. Therapeutic targets of neuroprotection and
671 neurorestoration in ischemic stroke: Applications for natural compounds from
672 medicinal herbs. Biomedicine & pharmacotherapy = Biomedecine &
673 pharmacotherapie. 2022; 148: 112719.

674 9. Zhu T, Wang L, Feng Y, Sun G, Sun X. Classical Active Ingredients and Extracts
675 of Chinese Herbal Medicines: Pharmacokinetics, Pharmacodynamics, and
676 Molecular Mechanisms for Ischemic Stroke. Oxidative medicine and cellular
677 longevity. 2021; 2021: 8868941.

678 10. Xie W, Zhu T, Dong X, Nan F, Meng X, Zhou P, et al. HMGB1-triggered
679 inflammation inhibition of notoginseng leaf triterpenes against cerebral ischemia
680 and reperfusion injury via MAPK and NF-κB signaling pathways. Biomolecules.
681 2019; 9.

682 11. Xie W, Zhu T, Zhou P, Xu H, Sun X. Notoginseng Leaf Triterpenes ameliorates
683 Mitochondrial Oxidative Injury via the NAMPT-SIRT1/2/3 Signaling Pathways
684 in Cerebral Ischemic Model Rats. Journal of ginseng research. 2020.

12. Xie W, Zhu T, Zhou P, Xu H, Meng X, Ding T, et al. Notoginseng Leaf Triterpenes Ameliorates OGD/R-Induced Neuronal Injury via SIRT1/2/3-Foxo3a-MnSOD/PGC-1α Signaling Pathways Mediated by the NAMPT-NAD Pathway. Oxidative medicine and cellular longevity. 2020; 2020: 7308386.

13. Yang K, Zhang H, Luo Y, Zhang J, Wang M, Liao P, et al. Gypenoside XVII Prevents Atherosclerosis by Attenuating Endothelial Apoptosis and Oxidative Stress: Insight into the ERα-Mediated PI3K/Akt Pathway. International journal of molecular sciences. 2017; 18.

14. Yu Y, Wang M, Chen R, Sun X, Sun G, Sun X. Gypenoside XVII protects against myocardial ischemia and reperfusion injury by inhibiting ER stress-induced mitochondrial injury. Journal of ginseng research. 2021; 45: 642-53.

15. Meng X, Wang M, Sun G, Ye J, Zhou Y, Dong X, et al. Attenuation of Aβ25-35-induced parallel autophagic and apoptotic cell death by gypenoside XVII through the estrogen receptor-dependent activation of Nrf2/ARE pathways. Toxicology and applied pharmacology. 2014; 279: 63-75.

16. Meng X, Luo Y, Liang T, Wang M, Zhao J, Sun G, et al. Gypenoside XVII Enhances Lysosome Biogenesis and Autophagy Flux and Accelerates Autophagic

703 Clearance of Amyloid-β through TFEB Activation. Journal of Alzheimer's
704 disease : JAD. 2016; 52: 1135-50.
705 17. Zhou J, Yao W, Li C, Wu W, Li Q, Liu H. Administration of follicle-stimulating
706 hormone induces autophagy via upregulation of HIF-1α in mouse granulosa cells.
707 Cell death & disease. 2017; 8: e3001.
708 18. Shi RY, Zhu SH, Li V, Gibson SB, Xu XS, Kong JM. BNIP3 interacting with
709 LC3 triggers excessive mitophagy in delayed neuronal death in stroke. CNS
710 neuroscience & therapeutics. 2014; 20: 1045-55.
711 19. Li PH, Zhao HC, Yan H. The main active components and pharmacological
712 research progress of the stems and leaves of *Panax notoginseng*. Guiyang
713 College of Traditional Chinese Medicine. 2006; 28: 49-52.
714 20. Huang Z, Luo X, Zhang Y, Ying Y, Cai X, Lu W, et al. Notoginseng Triterpenes
715 Inhibited Autophagy in Random Flaps via the Beclin-1/VPS34/LC3 Signaling
716 Pathway to Improve Tissue Survival. Frontiers in bioengineering and
717 biotechnology. 2021; 9: 771066.
718 21. Cui J, Gong R, Hu S, Cai L, Chen L. Gambogic acid ameliorates
719 diabetes-induced proliferative retinopathy through inhibition of the
720 HIF-1α/VEGF expression via targeting PI3K/AKT pathway. Life sciences. 2018;

721 192: 293-303.

722 22. Lv B, Li F, Han J, Fang J, Xu L, Sun C, et al. Hif-1α Overexpression Improves
723 Transplanted Bone Mesenchymal Stem Cells Survival in Rat MCAO Stroke
724 Model. Frontiers in molecular neuroscience. 2017; 10: 80.

725 23. Yang XS, Yi TL, Zhang S, Xu ZW, Yu ZQ, Sun HT, et al. Hypoxia-inducible
726 factor-1 alpha is involved in RIP-induced necroptosis caused by in vitro and in
727 vivo ischemic brain injury. Scientific reports. 2017; 7: 5818.

728 24. Chang Y, Hsieh CY, Peng ZA, Yen TL, Hsiao G, Chou DS, et al. Neuroprotective
729 mechanisms of puerarin in middle cerebral artery occlusion-induced brain
730 infarction in rats. Journal of biomedical science. 2009; 16: 9.

731 25. Bellot G, Garcia-Medina R, Gounon P, Chiche J, Roux D, Pouysségur J, et al.
732 Hypoxia-induced autophagy is mediated through hypoxia-inducible factor
733 induction of BNIP3 and BNIP3L via their BH3 domains. Molecular and cellular
734 biology. 2009; 29: 2570-81.

735 26. Lim JH, Lee YM, Chun YS, Chen J, Kim JE, Park JW. Sirtuin 1 modulates
736 cellular responses to hypoxia by deacetylating hypoxia-inducible factor 1alpha.
737 Molecular cell. 2010; 38: 864-78.

738 27. Rouble AN, Storey KB. Characterization of the SIRT family of

NAD+-dependent protein deacetylases in the context of a mammalian model of hibernation, the thirteen-lined ground squirrel. Cryobiology. 2015; 71: 334-43.

28. Verdin E, Hirschey MD, Finley LW, Haigis MC. Sirtuin regulation of mitochondria: energy production, apoptosis, and signaling. Trends in biochemical sciences. 2010; 35: 669-75.

29. Ng F, Wijaya L, Tang BL. SIRT1 in the brain-connections with aging-associated disorders and lifespan. Frontiers in cellular neuroscience. 2015; 9: 64.

30. Huo L, Bai X, Wang Y, Wang M. Betulinic acid derivative B10 inhibits glioma cell proliferation through suppression of SIRT1, acetylation of FOXO3a and upregulation of Bim/PUMA. Biomedicine & pharmacotherapy = Biomedecine & pharmacotherapie. 2017; 92: 347-55.

31. Yao CJ, Chow JM, Chuang SE, Chang CL, Yan MD, Lee HL, et al. Induction of Forkhead Class box O3a and apoptosis by a standardized ginsenoside formulation, KG-135, is potentiated by autophagy blockade in A549 human lung cancer cells. Journal of ginseng research. 2017; 41: 247-56.

32. Fu B, Zhao J, Peng W, Wu H, Zhang Y. Resveratrol rescues cadmium-induced mitochondrial injury by enhancing transcriptional regulation of PGC-1α and SOD2 via the Sirt3/FoxO3a pathway in TCMK-1 cells. Biochemical and

biophysical research communications. 2017; 486: 198-204.

33. She DT, Wong LJ, Baik SH, Arumugam TV. SIRT2 Inhibition Confers Neuroprotection by Downregulation of FOXO3a and MAPK Signaling Pathways in Ischemic Stroke. Molecular neurobiology. 2018; 55: 9188-203.

34. Zhang YN, Chen BM, Gao Yang, Li RP. Role of FoxO3a transcription factor in oxidative stress. Journal of Medical Postgraduates. 2016; 29: 5.

35. Wang H, Quirion R, Little PJ, Cheng Y, Feng ZP, Sun HS, et al. Forkhead box O transcription factors as possible mediators in the development of major depression. Neuropharmacology. 2015; 99: 527-37.

36. Zhang C, Li C, Chen S, Li Z, Ma L, Jia X, et al. Hormetic effect of panaxatriol saponins confers neuroprotection in PC12 cells and zebrafish through PI3K/AKT/mTOR and AMPK/SIRT1/FOXO3 pathways. Scientific reports. 2017; 7: 41082.

37. Kume S, Uzu T, Horiike K, Chin-Kanasaki M, Isshiki K, Araki S, et al. Calorie restriction enhances cell adaptation to hypoxia through Sirt1-dependent mitochondrial autophagy in mouse aged kidney. The Journal of clinical investigation. 2010; 120: 1043-55.

38. Zhu T, Wang L, Tian F, Zhao X, Pu XP, Sun GB, et al. Anti-ischemia/reperfusion

injury effects of notoginsenoside R1 on small molecule metabolism in rat brain after ischemic stroke as visualized by MALDI-MS imaging. Biomedicine & pharmacotherapy = Biomedecine & pharmacotherapie. 2020; 129: 110470.

39. Meng X, Wang M, Wang X, Sun G, Ye J, Xu H, et al. Suppression of NADPH oxidase- and mitochondrion-derived superoxide by Notoginsenoside R1 protects against cerebral ischemia-reperfusion injury through estrogen receptor-dependent activation of Akt/Nrf2 pathways. Free radical research. 2014; 48: 823-38.

40. Wang L, Zhu T, Xu HB, Pu XP, Zhao X, Tian F, et al. Effects of notoginseng leaf triterpenes on small molecule metabolism after cerebral ischemia/reperfusion injury assessed using MALDI-MS imaging. Annals of translational medicine. 2021; 9: 246.

41. Bieber M, Gronewold J, Scharf AC, Schuhmann MK, Langhauser F, Hopp S, et al. Validity and Reliability of Neurological Scores in Mice Exposed to Middle Cerebral Artery Occlusion. Stroke. 2019; 50: 2875-82.

42. Zhu T, Wang L, Xie W, Meng X, Feng Y, Sun G, et al. Notoginsenoside R1 Improves Cerebral Ischemia/Reperfusion Injury by Promoting Neurogenesis via the BDNF/Akt/CREB Pathway. Frontiers in pharmacology. 2021; 12: 615998.

43. Jiang B, Li L, Chen Q, Tao Y, Yang L, Zhang B, et al. Role of Glibenclamide in

Brain Injury After Intracerebral Hemorrhage. Translational stroke research. 2017; 8: 183-93.

44. Zhu T, Xie WJ, Wang L, Jin XB, Meng XB, Sun GB, et al. Notoginsenoside R1 activates the NAMPT-NAD(+)-SIRT1 cascade to promote postischemic angiogenesis by modulating Notch signaling. Biomedicine & pharmacotherapy = Biomedecine & pharmacotherapie. 2021; 140: 111693.

45. Zhu T, Fang BY, Meng XB, Zhang SX, Wang H, Gao G, et al. Folium Ginkgo extract and tetramethylpyrazine sodium chloride injection (Xingxiong injection) protects against focal cerebral ischaemia/reperfusion injury via activating the Akt/Nrf2 pathway and inhibiting NLRP3 inflammasome activation. Pharmaceutical biology. 2022; 60: 195-205.

Supplementary Files

This is a list of supplementary files associated with this preprint. Click to download.

- SupFigure7.21.docx